

Supporting Information

Quantifying millisecond exchange dynamics in proteins by CPMG relaxation dispersion NMR using side-chain ^1H probes

Alexandar L. Hansen, Patrik Lundström, Algirdas Velyvis, and Lewis E. Kay

Complete reference 18: Shen, Y.; Lange, O.; Delaglio, F.; Rossi, P.; Aramini, J. M.; Liu, G.; Eletsky, A.; Wu, Y.; Singarapu, K. K.; Lemak, A.; Ignatchenko, A.; Arrowsmith, C. H.; Szyperski, T.; Montelione, G. T.; Baker, D.; Bax, A. *Proc. Natl. Acad. Sci. U.S.A.* **2008**, *105*, 4685-90.

Conditions for Over-Expression of Fractionally Deuterated Samples: U- $\{{}^{13}\text{C}, {}^{15}\text{N}\}$, fractionally ^2H labeled wild-type Im7 protein was expressed using a pTrc99-A (Pharmacia) based expression vector¹ with BL21-CodonPlus(DE3)-RIL competent cells (Stratagene). The cells were grown in M9 minimal media with 1 g/L ${}^{15}\text{NH}_4\text{Cl}$ and 3 g/L U- $\{{}^{13}\text{C}, {}^1\text{H}\}$ -glucose as the sole nitrogen and carbon sources, respectively, 97% D_2O solvent, using the antibiotics chloramphenicol and carbenicillin. The cells were grown at 37°C to an OD of \approx 1.0 before induction with 1 mM IPTG and protein expression was allowed to continue overnight at room temperature to a final OD of \approx 3.0. Purification followed the same procedure as described previously². Although we have used 97% D_2O as solvent for protein overexpression, estimated by NMR based on the intensity of the

residual HDO/H₂O resonance, we would recommend using 99% D₂O in subsequent growths so as to increase the level of deuteration as much as possible.

Evaluating the Level of Protonation/Deuteration in Proteins Produced using D₂O, {¹³C,¹H}-Glucose: The expression of proteins in D₂O using fully protonated glucose as the sole carbon source has been described by Shekhtman *et al.*³ as an approach for producing fractionally deuterated proteins for structural studies. These authors established that the level of deuteration at the C^α position was in excess of 95% on average and that the total incorporation of deuterium, while amino acid specific, ranges from 70-80% at the non-exchangeable positions. Subsequently, Mulder and coworkers have reported a detailed analysis of the level of protonation in methyl containing side-chains of proteins that have been expressed using this labeling approach⁴. They have also established the utility of samples generated in this manner for ¹H CPMG relaxation dispersion studies focusing on ¹³CHD₂ methyl groups⁵. As described in the text the pulse scheme of Figure 2 allows for the simultaneous measurement of ¹H dispersion profiles at the β positions of Asx, Cys, Ser, His, Phe, Tyr and Trp as well as the γ positions of Glx, in addition to the methyl side-chain moieties. We restrict our focus here to the labeling patterns for the non-methyl side-chains that are of interest in the present study and refer the reader to the reference by Otten *et al*⁴ for a similar description for methyl containing residues.

Initially experiments were performed to establish the level of ‘enrichment’ of CHD methylene groups for the sites that are probed by the CPMG ¹H dispersion experiment described here. Clearly high levels of enrichment are desired to maximize sensitivity. A pair of samples of Im7 has been prepared, the first fully ¹³C and ¹H labeled, referred to as sample A in what follows, while a second sample was generated using D₂O, {¹³C,¹H}-glucose (sample B, the ¹H relaxation

dispersion sample'; see above for details of sample growth). Both samples are also fully ^{15}N labeled so that differences in sample concentrations can be easily assessed and taken into account by quantifying intensities in $^{15}\text{N}, ^1\text{H}$ correlation maps of each. Constant-time $^{13}\text{C}-^1\text{H}$ HSQC spectra^{6,7} were recorded under conditions where the effects of chemical exchange are minimal (25°C, pH 8.0, H₂O). In the case of sample A only a single set of cross peaks are observed since the protein is completely protonated. In contrast, spectra recorded on sample B show the characteristic isotope shifted correlations that correspond, in the case of methylene groups, to peaks from CH₂ and CHD correlations. It is possible to separate correlations from the different isotopomers on the basis of significant isotope shifts (approximately 0.31 ppm, 0.018 ppm in the ^{13}C and ^1H dimensions, respectively) or alternatively to record spectra that select either CH₂ or CHD moieties (we have done both). For a given residue type (Aromatic, Asx, Cys, Glx, Ser), the

fractional protonation at a position of interest is then given by $f = \frac{1}{N} \sum_i \frac{I_B^i}{I_A^i}$, where $I_j^i, j \in \{A, B\}$

is the volume of the i correlation of sample j that has been suitably normalized by the intensity of cross-peaks in the ^{15}N spectrum (i.e., the protein concentration) and N is the number of cross-peaks that are compared. In this manner it is possible to calculate, for sample B, both f_{CH_2} and the fractional incorporation of HD in the methylene group. The latter is defined as $f_{CHD} + f_{CDH}$, where f_{CHD} and f_{CDH} , assumed equal in the analysis, are the fraction of HD methylene groups with H in the pro-*R* and pro-*S*, positions. Thus, a fractional HD incorporation of 50% means that 25% of the methylene groups at a particular site contain H in the pro-*R* and 25% in the pro-*S* positions, respectively.

While it is important that the fractional enrichment of CHD moieties at the sites of interest be as high as possible it is also critical that a high level of deuteration be achieved at the α - (Asx, Cys, Ser, His, Phe, Tyr and Trp) or β - (Glx) positions proximal to the proton sites that are

studied. The fractional level of protonation at the C^α position, f_α , was obtained by comparing

cross-peak volumes in constant-time $^{13}\text{C}, ^1\text{H}$ correlation maps, with f_α calculated as $f_\alpha = \frac{1}{N} \sum_i \frac{I_B^i}{I_A^i}$,

described above. An average value (± 1 standard deviation) of $3.9 \pm 1.2\%$ is obtained, that is essentially invariant with amino-acid type, in good agreement with values reported previously^{3,4}.

In the case of Asx, Cys, Ser only the level of deuteration at the C^α position is of concern. This is also the case for the aromatic amino acids since the C^γ is a quaternary carbon so that three-bond $^1\text{H}-^1\text{H}$ couplings involving H^β protons are not an issue, while four- and five-bond couplings are in general very small (< 1 Hz). See for example, http://www.ebyte.it/library/educards/nmr/Nmr_ScalarRelaxation.html.

The level of protonation at the C^β position of Glx residues has been evaluated as described above with values of $f_{CH_2} \sim 0$ (not measurable) and $f_{CHD} + f_{CDH} = 0.14 \pm 0.06$ obtained. Thus, on average, 14%(86%) of Glx residues have a single(no) $^1\text{H}^\beta$ and we have noticed no signs of modulation due to scalar coupled magnetization transfer in ^1H dispersion experiments. The small level of fractional incorporation of protons at the β position (14% CHD, 86% CD₂) leads to a pair of isotope shifted C^γ, H^γ correlations in $^{13}\text{C}, ^1\text{H}$ spectra that we have used to cross-validate this result, Figure S1. C^γ, H^γ peaks associated with $C^\beta\text{HD}$ or $C^\beta\text{D}_2$ are well enough separated in spectra so that they can be fitted to extract relative volumes and hence $f_{CHD} + f_{CDH}$ values for the β position that are in good agreement ($0.10 \pm 0.01\%$) with those measured by comparing cross peaks from samples A and B (see above).

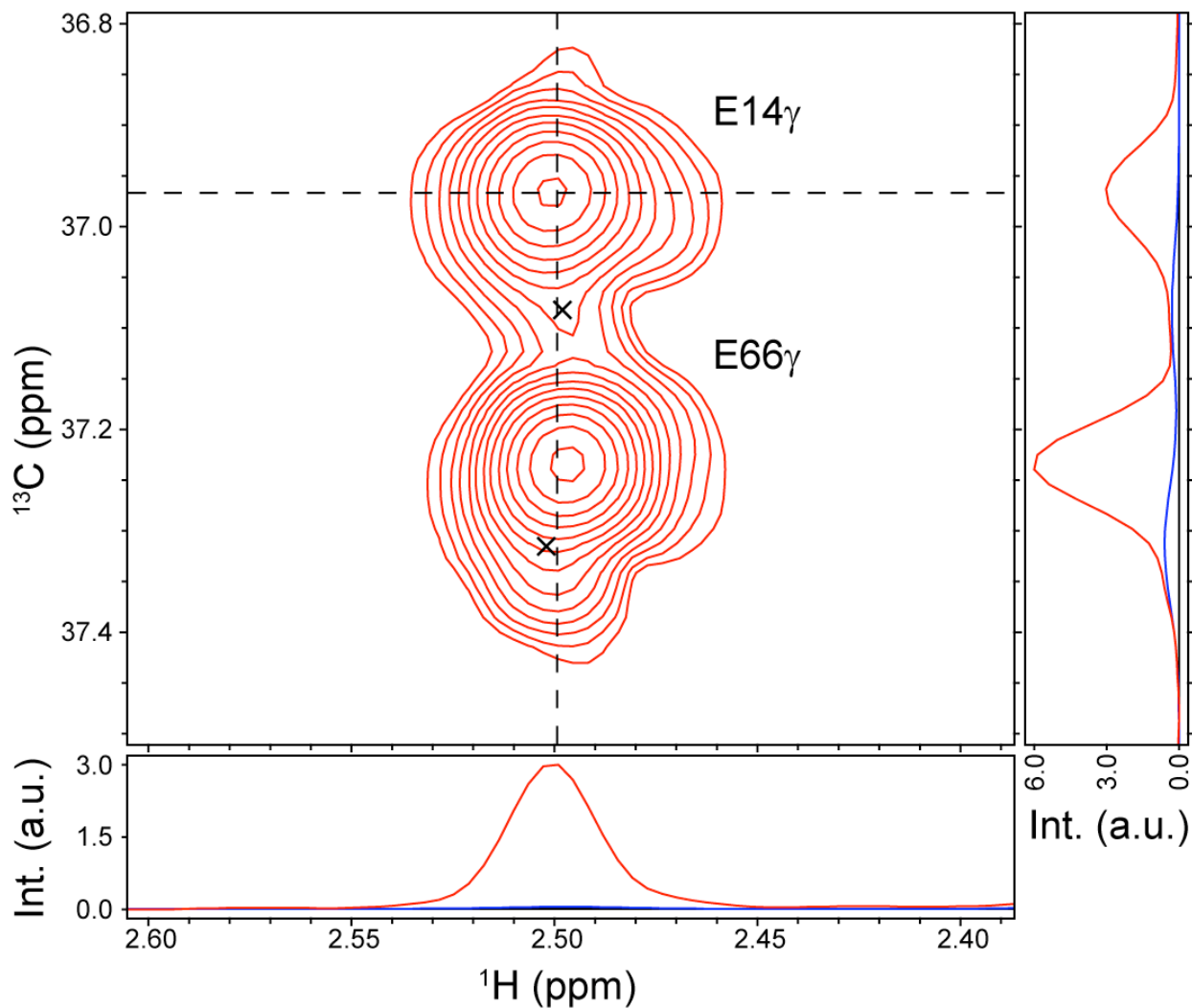


Figure S1. Selected region of ^{13}C , ^1H correlation spectrum recorded with the pulse scheme of Figure 2 ($T=0$), obtained by subtraction of the ‘Refocused’ and ‘Coupled’ data sets. Traces through the data are shown (red) along with the (small) contribution arising from protonation at the β position of the indicated Glu (blue, peak centered at x); the major peaks derive from C^γ carbons coupled to C^βD_2 . The volumes of the ‘blue’ peaks are 10% those of the major correlations.

Table 1B of the main text shows the experimentally derived f_{CH_2} and $f_{\text{CHD}}+f_{\text{CDH}}$ values for the sites in the ten non-methyl amino acids that are of interest. Notably, relatively good agreement between predicted and experimental $f_{\text{CHD}}+f_{\text{CDH}}$ values are obtained for Asx, Glx and Phe/Tyr while for Ser and Trp the level of incorporation is lower than expected. (Note, however,

the small N values for Trp that could account for some of the discrepancy for this residue; see discussion in text).

Suppression of Signals from Undesired Isotopomers: The goal is to suppress signals from isotopomers of the form $^{13}\text{CH}_3$ and $^{13}\text{CH}_2\text{D}$ (methyl groups) and $^{13}\text{CH}_2$ (methylenes) and in what follows we ‘trace’ magnetization from these moieties only. Immediately after the ^{13}C $90^\circ_{\phi_3}$ pulse of the scheme illustrated in Figure 2 the magnetization of interest is given by $2C_YI_Z$, where A_j ($j \in \{X, Y, Z\}$) is the j-component of A magnetization. During the subsequent τ_b period evolution due to the one-bond ^1H - ^{13}C scalar coupling proceeds according to

$$2C_YI_Z \rightarrow -3C_X \sin(\pi J_{HC}\tau_b) \cos^2(\pi J_{HC}\tau_b) - \{2 \sin(\pi J_{HC}\tau_b) \cos^2(\pi J_{HC}\tau_b) - \sin^3(\pi J_{HC}\tau_b)\} \sum_{i,j,i \neq j} 4C_X I_Z^i I_Z^j, \quad ^{13}\text{CH}_3$$

S1a

$$2C_YI_Z \rightarrow -C_X \sin(2\pi J_{HC}\tau_b) - 4C_X I_Z^i I_Z^j \sin(2\pi J_{HC}\tau_b), \quad ^{13}\text{CH}_2\text{D}, ^{13}\text{CH}_2$$

S1b

where the effects of relaxation are ignored and terms proportional to $2C_YI_Z$ ($^{13}\text{CH}_3$, $^{13}\text{CH}_2\text{D}$, $^{13}\text{CH}_2$) and $8C_YI_Z^1 I_Z^2 I_Z^3$ ($^{13}\text{CH}_3$) are not included in the above expressions as they are eliminated by the action of the $90_x 90_{\phi_4}$ purge element in concert with the phase cycle or by the 90_x purge and the subsequent coherence transfer selection gradients. Consider first the case of a $^{13}\text{CH}_3$ methyl group and the $90_x 90_{\phi_4}$ purge. Tracing the magnetization to the end of the CT period of Figure 2

and retaining only the dominant term that is proportional to $\sin^3(\pi J_{HC}\tau_b)$ since $\tau_b \approx \frac{1}{2J_{CH}}$, the

coherences of interest are given by $-2C_Y I_Z \sin^6(\pi J_{HC} \tau_b)$. That is, for $^{13}\text{CH}_3$ methyl groups the $90_x 90_{\phi 4}$ purge has little effect so that magnetization at the start and at the end of the CT element is essentially the same. By contrast, if instead only a 90° pulse is applied after an initial τ_b evolution period then the relevant terms immediately after the pulse are

$$\sin^3(\pi J_{HC} \tau_b) \sum_{i,j,i \neq j} 4C_X I_Y^i I_Y^j = 0.5 \sin^3(\pi J_{HC} \tau_b) \sum_{i,j,i \neq j} \{4C_X (I_Y^i I_Y^j + I_X^i I_X^j) + 4C_X (I_Y^i I_Y^j - I_X^i I_X^j)\}$$

S2

where the first and second terms in the summation denote zero- and double-quantum ^1H coherences, respectively. Only the zero-quantum component survives the coherence transfer selection gradients as they are calibrated to transfer ^{13}C transverse magnetization to ^1H (note that the gradients have no effect on ^1H zero-quantum coherences). It can be shown further that only a fraction of $4C_X (I_Y^i I_Y^j + I_X^i I_X^j)$ is transferred to observable magnetization at the end of the pulse scheme, giving rise to improved suppression relative to the $90_x 90_{\phi 4}$ element. A similar scenario holds also for the suppression of $^{13}\text{CH}_2\text{D}$ moieties. The $90_x 90_{\phi 4}$ purge has no effect on magnetization denoted by C_X and $4C_X I_Z^i I_Z^j$ (right hand side of eq S1b, $2C_Y I_Z$ is suppressed); both of these terms evolve to become observable magnetization. In contrast, in the case where the 90_x purge is used instead, $4C_X I_Z^i I_Z^j$ is suppressed (second term of the right hand side of eq S1b).

We have observed no difference between levels of suppression for $^{13}\text{CH}_2$ methylene groups using either of the two approaches for any of the residue types with the exception of Ser (see below), because a τ_b value can be chosen that efficiently eliminates the terms of eq S1b (*i.e.*, the range of J_{HC} values is small for the methylene groups in question). Ser is the exception because J_{HC} is considerably larger than for the other residues (147 Hz vs 130 Hz) so that the

S7

terms in eq S1b become more critical. In particular, when the 90° purge element is employed additional correlations are created in the “Coupled spectrum” at F_1 frequencies of $\omega_C \pm \omega_\Delta$, where ω_C is the ^{13}C Larmor frequency and ω_Δ is the frequency difference between the methylene proton spins in the $^{13}\text{CH}_2$ group of interest. These peaks arise because the 90° purge creates zero-quantum coherences (the double quantum elements are eliminated by the coherence transfer gradient pair) that evolve due to ^1H chemical shift during the CT period. Interestingly, the “Refocused” spectrum does not show these correlations because the placement of ^1H 180° pulses is such that ^1H chemical shift evolution is completely refocused. For Ser residues and where the 90° purge is employed, the ‘Refocused’ spectrum can be used by itself to generate dispersion profiles from peak intensities as a function of v_{CPMG} if these additional peaks interfere with quantitation of the correlations of interest.

To summarize, we have found that the levels of suppression of $^{13}\text{CH}_2\text{D}$ and $^{13}\text{CH}_3$ isotopomers are higher for the 90° purge relative to $90_x 90_{\phi 4}$. In the case of methylene groups both schemes are equally effective in suppressing $^{13}\text{CH}_2$ moieties for all residues except Ser where additional correlations are observed in the ‘Coupled’ spectrum, as described above. In the experiments described here we have used the $90_x 90_{\phi 4}$ element.

References

- (1) Le Duff, C. S.; Whittaker, S. B.; Radford, S. E.; Moore, G. R. *J Mol Biol* **2006**, 364, 824-35.
- (2) Hansen, A. L.; Kay, L. E. *J Biomol NMR* **2011**, 50, 347-55.

(3) Shekhtman, A.; Ghose, R.; Goger, M.; Cowburn, D. *FEBS Lett* **2002**, *524*, 177-82.

(4) Otten, R.; Chu, B.; Krewulak, K. D.; Vogel, H. J.; Mulder, F. A. *J Am Chem Soc* **2010**, *132*, 2952-60.

(5) Otten, R.; Villali, J.; Kern, D.; Mulder, F. A. *J Am Chem Soc* **2010**, *132*, 17004-14.

(6) Vuister, G. W.; Bax, A. *J. Magn. Reson.* **1992**, *98*, 428-435.

(7) Santoro, J.; King, G. C. *J. Magn. Reson.* **1992**, *97*, 202-207.